Journal of Controlled Release 342 (2022) 189–200

Contents lists available at ScienceDirect

Journal of Controlled Release

journal homepage: www.elsevier.com/locate/jconrel

Development of hot-melt extruded drug/polymer matrices for sustained delivery of meloxicam

Yun-Chu Chen [a], Dana E. Moseson [a], Coralie A. Richard [b], Monica R. Swinney [c], Sarena D. Horava [c], Kaoutar Abbou Oucherif [c], Amy L. Cox [b], Eric D. Hawkins [b], Yongzhe Li [a,d], Daniel F. DeNeve [a], Joshua Lomeo [e], Aiden Zhu [e], L. Tiffany Lyle [f], Eric J. Munson [a], Lynne S. Taylor [a], Kinam Park [a,g], Yoon Yeo [a,g,*]

[a] Department of Industrial and Physical Pharmacy, Purdue University, 575 Stadium Mall Drive, West Lafayette, IN 47907, USA
[b] Eli Lilly and Company, 893 Delaware Street, Indianapolis, IN 46225, USA
[c] Eli Lilly and Company, 450 Kendall Street, Cambridge, MA 02142, USA
[d] Department of Pharmaceutics, School of Pharmacy, Shenyang Pharmaceutical University, 103 Wenhua Road, Shenyang, Liaoning 110016, PR China
[e] DigiM Solution LLC, 67 South Bedford Street, West Burlington, MA 01803, USA
[f] Department of Comparative Pathobiology, Purdue University, 625 Harrison Street, West Lafayette, IN 47907, USA
[g] Weldon School of Biomedical Engineering, Purdue University, West Lafayette, IN 47907, USA

ARTICLE INFO

Keywords:
Meloxicam
Hot-melt extrusion
Sustained drug delivery
Biocompatible polymer
Implant

ABSTRACT

For effective resolution of regional subacute inflammation and prevention of biofouling formation, we have developed a polymeric implant that can release meloxicam, a selective cyclooxygenase (COX)-2 inhibitor, in a sustained manner. Meloxicam-loaded polymer matrices were produced by hot-melt extrusion, with commercially available biocompatible polymers, poly(ε-caprolactone) (PCL), poly(lactide-co-glycolide) (PLGA), and poly (ethylene vinyl acetate) (EVA). PLGA and EVA had a limited control over the drug release rate partly due to the acidic microenvironment and hydrophobicity, respectively. PCL allowed for sustained release of meloxicam over two weeks and was used as a carrier of meloxicam. Solid-state and image analyses indicated that the PCL matrices encapsulated meloxicam in crystalline clusters, which dissolved in aqueous medium and generated pores for subsequent drug release. The subcutaneously implanted meloxicam-loaded PCL matrices in rats showed pharmacokinetic profiles consistent with their *in vitro* release kinetics, where higher drug loading led to faster drug release. This study finds that the choice of polymer platform is crucial to continuous release of meloxicam and the drug release rate can be controlled by the amount of drug loaded in the polymer matrices.

1. Introduction

Inflammation is an important response to tissue injury and infection, which helps to control foreign stimuli and promote tissue repair. However, prolonged inflammation that is not resolved for weeks to months can cause tissue damage, translating to chronic inflammatory diseases. Non-steroidal anti-inflammatory drugs (NSAIDs) are commonly used for treatment of inflammation. NSAIDs reduce the synthesis of prostaglandins, lipid inflammatory mediators derived from arachidonic acid [1], by inhibiting catalytic enzymes of the synthetic pathway, such as cyclooxygenase (COX)-1 and COX-2 [2]. NSAIDs are typically administered as oral drugs; however, a variety of side effects, including vomiting, heartburn, headache, depression, gastrointestinal ulceration, and heart attack, have prohibited their chronic use [3,4]. The high incidence of side effects has prompted the development of specialized formulations of NSAIDs based on nano- or microparticles, which add a contact barrier between the drug and off-target sites and/or control the drug release kinetics [5–7]. However, oral administration, even with special formulations, does not completely eliminate systemic side effects of NSAIDs, even with the encapsulation. Therefore, when inflammation is regionally confined as in arthritis and periodontal diseases, local delivery of NSAIDs by implantable devices such as hydrogels [8] or polymeric structures [9,10] is a reasonable alternative. Locally implantable devices that can release NSAIDs in a sustained manner can reduce systemic drug exposure and the frequency of administration, thereby improving the patient's experience and adherence to the regimen.

* Corresponding author at: Department of Industrial and Physical Pharmacy, Purdue University, 575 Stadium Mall Drive, West Lafayette, IN 47907, USA.
E-mail address: yyeo@purdue.edu (Y. Yeo).

https://doi.org/10.1016/j.jconrel.2021.12.038
Received 22 June 2021; Received in revised form 2 November 2021; Accepted 29 December 2021
Available online 3 January 2022

Meloxicam is a relatively selective COX-2 inhibitor, indicated for the treatment of rheumatoid arthritis, osteoarthritis, ankylosing spondylitis, joint pain, and post-surgical inflammation [11,12]. Due to the selectivity, meloxicam shows a more favorable safety profile than non-selective NSAIDs [13,14]. Studies have also shown an anti-tumor effect of meloxicam against ovarian cancer and colorectal cancer, due to the involvement of COX-2 in the progression of these cancers [15,16]. Moreover, meloxicam has been found to be useful in the prevention of biofilm formation on implanted devices or post-surgical wound dressings, where meloxicam reduces the production of extracellular polysaccharides, DNA, and quorum-sensing virulence factors [17]. The diverse therapeutic functions of meloxicam in regional complications motivate the development of a sustained local delivery system. At present, meloxicam is mostly available as an oral formulation [18–21], although other routes of administration such as intravenous [22], ocular [23], vaginal [24] and rectal [25] have been used or tested in clinical trials. Most of the parenteral meloxicam formulations are to treat pain at the systemic level, but meloxicam has also been pursued for prolonged management of local inflammation. For instance, an *in-situ* gelling formulation based on poly(oxyethylene)-poly(oxypropylene) block copolymer was developed to prolong the meloxicam release for 7 days for local treatment of periodontitis, showing clinical improvement in pocket depth and bone density [26].

In this study, we aim to develop a polymeric matrix for sustained delivery of meloxicam over two weeks, which may be implanted or fabricated into a wound dressing for prevention of subacute inflammation and biofouling formation. Subacute inflammation is an intermediate stage linking acute inflammation to chronic inflammation that lasts 2 to 6 weeks [27]. Biofilms take up to 2 weeks from bacterial seeding to form microcolonies, which then mature to structured matrices with extracellular polymer substances [28]. Therefore, controlled release of meloxicam over at least 2 weeks is critical to the success of wound management. We have screened commercially available biocompatible polymers to identify a polymer suitable for 2-week sustained delivery of meloxicam. We produce meloxicam-loaded polymer matrices by hot-melt extrusion (HME), evaluate the release kinetics *in vitro* and *in vivo*, and characterize the matrices using scanning electron microscopy (SEM), electron dispersive x-ray analysis (EDX), micro-computed tomography (microCT), X-ray powder diffraction (XRPD), and differential scanning calorimetry (DSC) to understand how the encapsulating polymer affects meloxicam release. Our study finds that poly(ε-caprolactone) (PCL) is suitable for 2-week sustained release of meloxicam. PCL matrices control meloxicam release by encapsulating the drug in clusters, which dissolve in water and generate pores for subsequent drug release. Pharmacokinetics of subcutaneously implanted meloxicam-PCL matrices in rats show that *in vivo* drug release and absorption occur in the rank order predicted *in vitro*.

2. Materials and methods

2.1. Materials

Poly(ε-caprolactone) (PCL; Purasorb PC 17 and Resomer® C 212) and poly(lactide-*co*-glycolide), also known as poly(L-lactic-*co*-glycolic acid) (PLGA, Resomer® RG502, LG 855 S and LG 824 S), tetrahydrofuran (THF) and Trizma base were obtained from Sigma-Aldrich (MilliporeSigma, Burlington, MA, USA). Poly(ethylene vinyl acetate) (EVA; Ateva 2803G, 28% vinyl acetate) was a gift of Celanese (Dallas, TX). Meloxicam (lot 2690001Y03F, 100.6% potency) was obtained from Olon Derivados Quimicos (Alcantarilla, Spain). Solid state properties of meloxicam and polymers are listed in Supporting Table 1. Dimethyl sulfoxide (DMSO, Fisher Chemical), phosphate buffered saline (PBS Tablets, Fisher Bio Reagents), and Tween 80 (Quality Biological Inc) were purchased from Fisher Scientific (Pittsburgh, PA).

2.2. Measurement of meloxicam solubility

To measure meloxicam solubility in PBST at 37 °C, >1 mg of meloxicam was dispersed in 1 mL of PBST and agitated by bath sonication and vortex mixing for 10 min each. The insoluble meloxicam was removed by centrifugation at 9800 xg, the supernatant was filtered through a 0.25 μm syringe filter and analyzed by HPLC (Section 2.9). For measuring meloxicam solubility in different pHs, 1 mg of meloxicam was dispersed in 1 mL PBS, and the pH of the suspension was adjusted to pH 4, 5, or 7.4 with diluted HCl as needed. After centrifugation, the supernatant was sampled, diluted with DMSO, treated and analyzed as described above. All samples were prepared in triplicate.

2.3. Preparation of meloxicam/polymer matrices

Meloxicam/polymer HME matrices were prepared with an Xplore Pharma Melt Extruder (Geleen, The Netherlands), assembled with a 2 mL volume barrel and co-rotating screws varying the processing parameters as summarized in Table 1. The screws were rotated at 20 rpm, except for selected studies. Each batch contained a total of 3.5 g of meloxicam and polymer mixture, varying the wt% of meloxicam. Meloxicam was received as a micronized powder with a volume moment mean diameter D [3,4] of 7.46 ± 0.33 μm, measured by a Mastersizer 3000 particle size analyzer (Malvern, Worcestershire, UK). Meloxicam and polymers were mixed and extruded as received, without milling or pre-processing, through a die with a diameter of 2 mm. The matrices were named according to the meloxicam content and the type of polymer: for example, PLGA RG502 matrix with 10 wt% meloxicam as M10/PLGA RG502. Unless specified otherwise, PCL refers to PCL PC17. Therefore, PCL PC17 matrices with 30, 40, 50 and 65 wt% meloxicam are called M30/PCL, M40/PCL, M50/PCL, and M65/PCL, respectively.

Table 1
Processing parameters of HME meloxicam/polymer matrices.

HME matrices	Polymer	Drug loading[1] (wt%)	Operating set temp (°C)	Product melt temp (°C)	Residence time[2] (min)
M10/PLGA RG502	PLGA RG502	10%	185 ± 1	180 ± 1	5
M10/PLGA RG855	PLGA RG855	10%	185 ± 1	180 ± 1	1.5
M10/PLGA RG824	PLGA RG824	10%	185 ± 1	180 ± 1	6
M10/EVA 2803G	EVA 2803G	10%	155 ± 1	150 ± 1	2
M10/PCL	PCL PC17	10%	135 ± 1	130 ± 1	4
M10/PCL C212	PCL C212	10%	135 ± 1	130 ± 1	4
M30/PLGA RG502	PLGA RG502	30%	105 ± 1	100 ± 1	6
M30/PCL	PCL PC17	30%	110 ± 1	105 ± 1	4
M40/PCL	PCL PC17	40%	115 ± 1	110 ± 1	4
M50/PCL	PCL PC17	50%	120 ± 1	115 ± 1	4
M65/PCL	PCL PC17	65%	125 ± 1	120 ± 1	4

[1] Drug loading (wt%) = Weight percentage of meloxicam in the total meloxicam-polymer mixture.
[2] Residence time refers to the time when the recirculation valve is opened and the melt begins extruding. The total extrusion time ranged from 1 to 6 min later, depending on material flow properties.

2.4. Water contact angle measurement

Water contact angles on polymeric matrices were measured by a Ramé-Hart Model 200 Goniometer/Tensiometer (Ramé-Hart Instrument co, Succasunna, NJ, USA). Deionized water (1 μL) was placed onto different locations on the surface of PCL, PLGA and EVA HME matrices with or without 30 wt% meloxicam, and their optical images were acquired. The contact angles of the droplets were determined by a DROPimage Pro software (Ramé-Hart Instrument co, Succasunna, NJ, USA) and reported as an average of three measurements.

2.5. SEM/EDX analysis

The surface and cross-sections of meloxicam/PCL matrices were analyzed by SEM, combined with EDX, to visualize drug distribution in the matrices. The matrices were attached to an aluminum stub and sputter-coated with a thin platinum layer (Turbo-Pumped Sputter, Cressington Scientific Instruments, Watford, UK) at 40 mA for 60 s. The exterior and interior (cut open by a razor blade) surfaces of the matrices were visualized with an FEI NOVA nanoSEM Field Emission SEM (FEI Company, OR, USA) at an acceleration voltage of 7 kV, working distance of 5 mm, and spot size of 4.5. Elemental distribution in the matrices was determined by EDX with an Oxford INCA Xstream-2 silicon drift detector, run in mapping mode with an Xmax80 window at a magnification of 20,000×, and analyzed by AZtecOne software (Oxford Instrument, Abingdon, UK).

2.6. X-ray MicroCT analysis

A SkySkan 1272 MicroCT scanner (Bruker, Manning Park, MA) was used to investigate the internal structure of meloxicam/PCL PC17 matrices after preparation and after release studies (see Section 2.9). The CT images were obtained with an X-ray tube voltage of 40 kV, a tube current of 250 μA, a 0.5 mm aluminum beam filter, a frame averaging of 4, and a random movement of 60. An M65/PCL cut by a stainless blade (length: 1.5 cm; diameter: ~2 mm) was mounted on a Styrofoam holder with a rotating stage over 180° and a rotation step of 0.2°. The spatial resolution was 2.5 μm/pixel. The DigiM I2S software platform was utilized for image reconstruction and artificial intelligence (AI) segmentation to classify phases [29]. The AI segmentation module applied a user-input training to label voxels based on their grayscale intensity and morphological features. A thickness distribution module in I2S was used to measure the thickness of an outer porous layer observed in microCT scans [30]. 3D Slicer was implemented to generate 3D visualizations of AI segmented datasets [31].

2.7. XRPD analysis

PCL PC17 and meloxicam/PCL matrices were analyzed by X-ray powder diffraction (XRPD). Approximately 5 g of the sample was milled in liquid nitrogen by the 6750 Freezer/Mill (SPEX, Metuchen, NJ) at 10 Hz for a total of 4 min. XRPD patterns of cryo-milled meloxicam/PCL matrices, physical mixtures, and individual components were collected using a Rigaku SmartLab diffractometer (Rigaku Americas, The Woodlands, Texas) in Bragg-Brentano mode with a Cu-Kα radiation source and a d/tex ultra detector. The patterns of the powdered meloxicam/PCL matrices and raw materials were obtained from 5 to 40° 2θ with a 10°/min scan rate using a glass sample holder.

2.8. DSC analysis

A Q2000 differential scanning calorimeter (DSC) equipped with a refrigerated cooling accessory (TA Instruments, New Castle, DE) purged with nitrogen at 50 mL/min was used to characterize the solid state of raw materials and cryomilled meloxicam/polymer HME matrices (M30/PCL, M40/PCL, M50/PCL, M65/PCL, M30/PLGA RG502 and M30/EVA). The cryomilled samples (3–5 mg) were loaded in standard aluminum pans. Meloxicam was heated at 10 °C/min until the melting point was detected. PCL PC17, PLGA RG502, EVA polymers and meloxicam/polymer HME matrices were heated up to 280 °C at 10 °C/min. Additionally, PCL PC 17 and M30/PCL, M40/PCL, M50/PCL and M65/PCL were heated from 0 °C to 200 °C at 10 °C/min, then cooled to 0 °C at 10 °C/min, followed by a second heating ramp to 200 °C at 10 °C/min.

2.9. In vitro meloxicam release kinetics

Each meloxicam/PCL matrix was cut to 0.8–2.5 mg (equivalent to ~660 μg meloxicam, in 2 mm diameter × variable lengths) and suspended in 20 mL PBS (10 mM phosphate, pH 7.4) containing 0.1% Tween 80 (PBST). The solubility of meloxicam in PBST at 37 °C was measured to be 99 ± 3 μg/mL (as described in Section 2.2). Thus, the ratio of matrix-to-release medium (660 μg meloxicam in 20 mL PBST) satisfies sink conditions (≤ 1/3 of saturation solubility [32–35]). Alternatively, the matrices were cut to the same geometry and dimension (2 mm diameter × 1 mm length) and suspended in varying volumes of PBST to satisfy sink conditions. The matrix was incubated at 37 °C on an orbital shaker at 15 rpm. At predetermined time points, 0.5 mL of the release medium was sampled for analysis, and the medium was replenished with 0.5 mL of fresh PBST. For selected cases, release studies were performed with PBST containing 50 mM phosphate to afford relatively high buffering capacity. The sampled medium was analyzed by high performance liquid chromatography (HPLC) to determine the concentration of meloxicam. An Agilent 1290 HPLC System (Agilent Technology, CA, USA), equipped with a 250 × 4.6 mm Luna 5 μm C18 reverse phase column (Phenomenex, CA, USA), 1290 Binary Pumps and a 1290 Variable Wavelength Detector, was run at 0.8 mL/min and room temperature over 15 min, with a mobile phase consisting of acetonitrile and 50 mM pH 6.5 phosphate buffer (30:70, *v*/v). The meloxicam signal was detected at 355 nm. The retention time of meloxicam was 10 min. Following the release kinetics study, the remaining solids were analyzed by SEM/EDX and microCT as described above. For quantifying unreleased meloxicam, the remaining matrices were dissolved in tetrahydrofuran (THF), extracted with two volumes of Tris buffer (10 mM, pH 8), and analyzed by HPLC.

2.10. Brunauer-Emmett-Teller (BET) and Barrett-Joyner-Halenda (BJH) analysis

The porosity of the meloxicam/PCL HME matrices having completed a 14-day release kinetics study was quantified by a Micromeritics ASAP 2020 Plus Physisorption (Norcross, GA, USA). The matrices were 2 cm in length (weighing between 0.156 and 0.244 g) and incubated in PBST for 14 days to release drug. The samples were vacuum dried, degassed down to an absolute pressure of 50 μmHg, and heated to 40 °C for 2 h to ensure the removal of residual moisture. The degassed samples were analyzed using nitrogen (99.995% purity) as the adsorbate gas within a controlled liquid nitrogen environment at 77 K. Free space was determined by measuring the free space of an empty analysis tube. A total of 45 adsorption and desorption points were taken from a relative pressure (P/P_0) of 0.01 to 0.998. At each relative pressure, the sample was equilibrated for five seconds prior to data collection. Five data points in the range of 0.05 to 0.3 P/P_0 were used to calculate the BET transform isotherm. Pore characteristics were determined using the BJH adsorption [36] and desorption isotherms over the P/P_0 range of 0.1 to 0.998.

2.11. Meloxicam pharmacokinetics from subcutaneously implanted M/PCL HME matrices

2.11.1. Study design

Male Sprague Dawley rats (~456 g) were purchased from Envigo (Indianapolis, IN) and group housed (2–3 per cage) at 22–25 °C with a

relative humidity of 45 ± 10% and a 12 h light–dark cycle. All procedures were in compliance with the ethical standards and guidelines issued by Eli Lilly's IACUC. The animals were divided into 8 groups (5 animals per group), where groups 1–4 received meloxicam HME matrices (1 matrix per rat), which weighed 8.4 ± 1.9 mg containing 30, 40, 50, or 65 wt% meloxicam (2.4–5.5 mg meloxicam). All animals underwent isoflurane anesthesia and were shaved and aseptically prepared with betadine and alcohol. The samples were implanted by making a 1 cm incision and placing in a small subcutaneous pocket on the scapular area of the animals' backs. The small incisions were closed with a single staple. Control groups (one group for early time point and the other for full sampling time points per each route) were injected with a single subcutaneous bolus injection or a tail vein intravenous (IV) injection of a commercial solution containing 2 mg meloxicam (Alloxate 5 mg/mL, Patterson Veterinary, Lot: 810392D). Blood samples were collected (100 μL) *via* a tail clip into EDTA at predefined time intervals. After 14 days, animals were sacrificed in their home cages by carbon dioxide euthanasia followed by cervical dislocation, and the implants were recovered and analyzed as described in Section 2.9 to quantify the unreleased drug.

2.11.2. Preparation and analysis of plasma calibration standards and samples

Plasma meloxicam levels were determined by LC Mass Spectrometry (Q2 Solutions, Indianapolis, IN). Stock solutions containing 1 mg/mL of meloxicam were diluted to produce working solutions, which were then used to fortify control plasma to produce calibration standards with concentrations ranging from 1 to 5000 ng/mL or 25 to 50,000 ng/mL. Aliquots of each study sample, calibration standard, and control samples were transferred to 96-well plates, mixed with acetonitrile/methanol (1:1, *v*/v) containing an internal standard to precipitate sample proteins, and then centrifuged to pellet insoluble materials. The resulting supernatants were diluted with water (10-fold) and chromatographically separated using a Sprite ECHELON C18 4 μm 20 × 2.1 mm (Flanders, NJ), with a gradient LC system composed of water/1 M NH_4HCO_3 (2000:10, v/v) (mobile phase A) and MeOH/1 M NH_4HCO_3 (2000:10, v/v) (mobile phase B). The gradient profile was at 40% B from 0 to 0.20 min, ramp to 70% B from 0.20 to 0.30 min, hold at 70% B from 0.30 to 0.40 min, ramp to 98% B from 0.40 to 0.41 min, and hold at 98% B from 0.41 to 0.72 min, at a flow rate of 1.5 mL/min. The chromatography was performed at ambient laboratory conditions, with the effluent directed to the mass spectrometer between 0.25 and 0.5 min. The LC-MS/MS analysis utilized an Applied Biosystems/MDS Sciex API 4000 (Foster City, CA) equipped with a Turbo Ion Spray interface, and operated in positive ion mode. The analyte was detected and quantified by Selected Reaction Monitoring (SRM) $(M + H)^+$ transitions (meloxicam, *m/z* 352.1 > 115.0). The mass spectrometer quadrupoles were tuned to achieve unit resolution (0.7 DA at 50% FWHM), and data were acquired and processed with Applied Biosystems/MDS Sciex Analyst software (version 1.6.3). Plasma concentration results were uploaded into the Oracle database Watson (Thermo Scientific).

2.11.3. Pharmacokinetics (PK) analysis

To assess the *in vivo* input rate (the rate of drug entering the systemic circulation) of meloxicam from the subcutaneously implanted HME matrices, a PK analysis of the plasma concentration profiles was performed for each formulation. The plasma profiles were deconvoluted using the deconvolution through convolution method in Phoenix® WinNonLin® (version 8.1.0, Certara L.P). Deconvolution was performed using individual drug plasma concentration values, where the unit impulse response (UIR) of each subject was convolved with an initially guessed subject input rate profile.

Assuming the PK characteristics of the drug response follow linearity and time invariance, the UIR is expressed as:

$$C_\delta(t) = \sum_{j=1}^{N} A_j e^{-\alpha_j t} \quad (1)$$

where C_δ is the plasma concentration as a function of time, A an empirical constant, α_j a hybrid rate constant of the distribution and elimination phases, and N the number of exponential terms. The IV bolus plasma profile represents the UIR; therefore, A and α_j were estimated by fitting the IV data using GastroPlus™ software (Simulations Plus, Inc., CA).

The deconvolution method consisted of three iterative steps: (i) adjustment of the input function by changing its parameter values, (ii) convolution of the new input function with C_δ *(t)* to generate a predicted plasma concentration time profile, (iii) a quantitative comparison of the difference between the observed and calculated drug plasma values, used in the 'corrector step' of the algorithm to modify the input rate of the drug. The three steps were repeated until the objective function was optimized by minimizing the difference between the calculated and absorbed values to the acceptable level of fit.

2.11.4. In vitro–in vivo correlations (IVIVC)

The average *in vivo* input profiles were compared with the corresponding average *in vitro* release profiles. The IVIVC analysis was conducted in Phoenix using the IVIVC Toolkit. First, the *in vitro* release data were used as inputs in the model. The profiles were fit using a Weibull function. The plasma concentration and dosing data were mapped to the IVIVC object. Then, a UIR function was determined using the mean concentration–time data following the administration of the IV bolus dose. The deconvolution step followed to compute the fraction absorbed over time and to perform numeric deconvolution. Finally, an IVIVC relationship between the fraction of drug released *in vitro* ($F_{rel,\ in\ vitro}$) and the fraction of drug absorbed *in vivo* ($F_{input,\ in\ vivo}$) was fitted to the data for each matrix. The internal predictability of the model was also evaluated, where the IVIVC model was used to predict each formulation's plasma concentration profile from the *in vitro* release kinetics of each matrix.

2.12. Histological evaluation of subcutaneous tissues implanted with M/PCL HME matrices

Male Sprague Dawley rats were subcutaneously implanted with M65/PCL HME matrices on one side and blank PCL HME matrices (no drug) on the contralateral side in the same way as Section 2.11. After 14 days, animals were sacrificed, and the skin through the muscle layer of the implanted location was excised in 10% neutral buffered formalin. An untreated skin/muscle layer was also excised for comparison. The sampled tissues were embedded in paraffin, sectioned, and stained with hematoxylin and eosin (H&E) for histological evaluation by a board-certified veterinary pathologist. The samples were imaged by an Olympus BX43 light microscope. The slides were digitized by the Aperio VERSA 8-slide scanner and Aperio ImageScope 12.3 and read by a board-certified veterinary pathologist blinded to the specimen identity.

3. Results

3.1. Selection of polymer matrix for 14-day delivery of meloxicam

PLGA, PCL, and EVA were considered as potential matrix candidates for their frequent use in medical device research [37–41]. Meloxicam/polymer HME matrices were produced at minimum temperatures at which drug and polymer could be co-extruded. The drug-loaded matrices were evaluated for *in vitro* drug release kinetics to determine the suitability for continuous release of meloxicam (Fig. 1a). Water contact angles and DSC thermograms of the drug/polymer matrices were measured to help interpret differential drug release kinetics.

We first measured the T_g and/or T_m of candidate polymers to

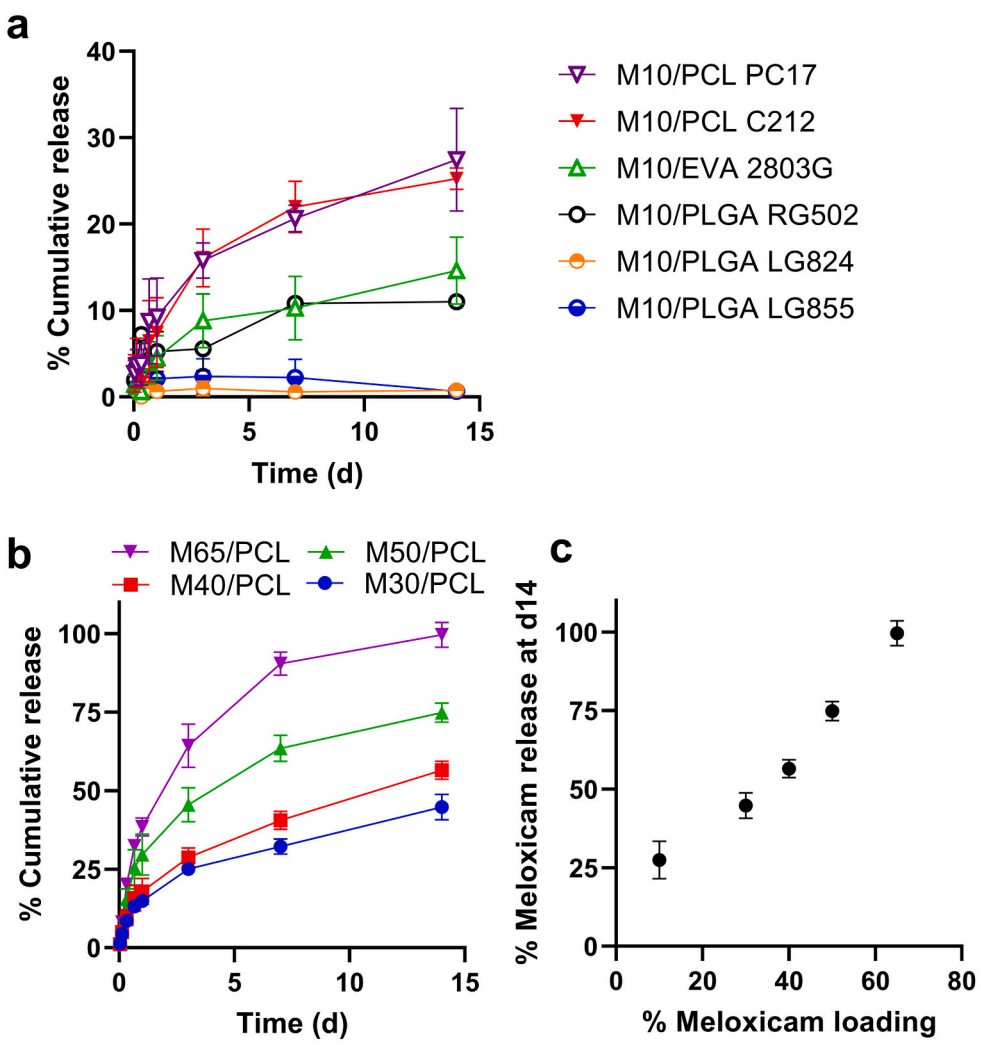

Fig. 1. (a) *In vitro* drug release profiles of hot-melt extruded polymer matrices with 10 wt% (M10) meloxicam loading. Mean ± standard deviation (SD), n = 3–4 replicates of a representative batch. (b) *In vitro* drug release profile of PCL PC17 matrices with 30, 40, 50 and 65 wt% meloxicam loading. Mean ± standard deviation (SD), n = 3 independently and identically prepared batches. (c) Correlation between % total meloxicam released in 14 days and wt% drug loading in PCL PC17 matrices. Mean ± SD, n = 3 independently and identically prepared batches, except for 10% loading, which is a mean ± SD of 4 replicates of a representative batch.

determine the HME conditions. PCL PC17 showed a T_m of 55–65 °C; PCL C212 showed a T_m of 55–70 °C; PLGA RG502 had a T_g of 46 °C (inflection point); PLGA LG824 and LG855 had a T_g of 58 °C (inflection point) and T_m of 149–162 °C and 157–167 °C, respectively; and EVA 2803G had a Tg of 38–44 °C and T_m of 73–84 °C (Supporting Fig. 1a), all consistent with the values provided by commercial sources (Supporting Table 1). Meloxicam had a melting temperature of 256.9 ± 0.7 °C (Supporting Fig. 1b). Since the melting temperature of meloxicam is close to or higher than thermal decomposition temperatures of the drug (~270 °C [42]) and PLGA (~220 °C, Supporting Fig. 1b), meloxicam and polymers were *co*-extruded at a temperature that each polymer could flow through the extruder (*i.e.*, T > T_m or T_g of each polymer) but meloxicam remained largely in the particle form as shown in the hot-stage microscopy images (Supporting Fig. 2).

M/PCL: M/PCL was extruded at 105–130 °C. PCL C212 and PC17 matrices with 10 wt% drug loading showed sustained drug release up to 25% and 27% release of the total loaded meloxicam, respectively, over 14 days (Fig. 1a). Increasing the meloxicam loading in the PCL PC17 matrix from 10 wt% to 65 wt% enhanced the cumulative amount of drug release from 27% to 100% of the total loaded drug, respectively, over 14 days (Supporting Fig. 3a). PCL PC17 matrix with 30 wt% meloxicam (M30/PCL) had a contact angle of 76°, lower than that of a neat polymer matrix (88.7°), and showed an even lower contact angle (71.2°) after 7 days of wetting in PBST (Supporting Fig. 4). The DSC thermogram of M30/PCL revealed no thermal events suggestive of molecular interaction between meloxicam and PCL up to the extrusion temperature (Supporting Fig. 1a). Upon further heating to >200 °C, DSC detected a slight depression of meloxicam melting temperature (Supporting Fig. 1b), suggesting partial mixing of meloxicam and PCL in the melt [43]. However, the partial mixing would be irrelevant to M/PCL matrices of this study, which were processed at a temperature < 130 °C. Therefore, the DSC results are consistent with the X-ray analysis in suggesting that meloxicam is present as the crystalline form in the matrices.

M/PLGA: M/PLGA was extruded at 100–180 °C. M10/PLGA RG502 showed an initial burst release in the first 16 h, reaching a plateau at 11% release of the total loaded meloxicam, with no further release for 14 days (Fig. 1a). An increase of meloxicam loading to 65 wt% did not increase drug release beyond 12% (Supporting Fig. 3a). M10/PLGA LG824 and M10/LG855 matrices showed negligible drug release in 14 days (Fig. 1a). M30/PLGA RG502 had contact angles of 65.4° and 58.2° as fresh or 7-day wet matrices, respectively, whereas neat PLGA RG502 showed 88.5°. The DSC thermogram showed no thermal events indicating molecular interaction between meloxicam and PLGA RG502 up to the extrusion temperature, except for a small exothermic event at 80 °C (Supporting Fig. 1b), which could not be related to any known phase transformation of either component. When further heated (>220 °C), PLGA degraded before one could observe any change in meloxicam melting temperature to infer drug-polymer interaction (Supporting Fig. 1b).

M/EVA: M/EVA was extruded at 150 °C. M10/EVA continuously but slowly released 15% of the total loaded meloxicam by day 14 (Fig. 1a).

M65/EVA released 35% of the loaded drug by day 14 (Supporting Fig. 3a). Neat EVA had a contact angle of 93.1°, and M30/EVA showed 101.9° and 81.8° as fresh or 7-day wet matrices, respectively, indicating hydrophobicity and minimal wetting of the matrix. The DSC thermogram showed no thermal event indicative of molecular interaction between meloxicam and EVA in the scanned temperature range (20–280 °C) (Supporting Fig. 1b).

3.2. In vitro meloxicam release kinetics from meloxicam/PCL matrices

Based on the initial screening, we chose PCL PC17 as a meloxicam carrier matrix to achieve sustained release over the course of 14 days. Since the initial assessment showed that drug release increased with drug loading (Supporting Fig. 3a), the HME matrices were prepared with drug loadings ranging from 30 wt% to 65 wt%. Meloxicam release from the M/PCL matrices was tested in PBST under sink conditions. There was a positive correlation between the fraction of released drug and the meloxicam loading content (Fig. 1b). M30/PCL, M40/PCL, M50/PCL, and M65/PCL matrices released 15%, 18%, 30% and 38% of the total loaded drug, respectively, in the first 24 h. Subsequently, all four matrices showed a continuous drug release, with M30/PCL, M40/PCL, M50 PCL, and M65/PCL releasing 45%, 57%, 75%, and 100% of the loaded drug, respectively, in 14 days (Fig. 1c). Since this study was performed with a fixed amount of meloxicam (*i.e.*, varying the length of the matrices), the release kinetics were repeated with matrices of fixed dimension (Supporting Fig. 5). The same trend was observed, indicating that the release rate was irrespective of the diffusion length in the matrix. Consistent with the complete drug release from M65/PCL, the yellow colour of meloxicam disappeared from the matrix after 14 days of release (Supporting Fig. 6). Mass balance confirmed that the remaining meloxicam in the M65/PCL sample was negligible (0.01%).

3.3. Solid state analysis of meloxicam/PCL HME matrices

X-ray powder diffraction (XRPD) was used to evaluate the solid state of meloxicam, PCL PC17, and M/PCL matrices (Fig. 2a). The diffractograms of M/PCL matrices showed the peaks of meloxicam and PCL physical mixtures, indicating that meloxicam retained its crystalline state and PCL PC17 recrystallized upon cooling after HME (Supporting Fig. 7). The diffraction intensities of fresh matrices reflected the relative proportion of crystalline meloxicam or PCL PC17 present in the matrices (Fig. 2a). M/PCL matrices showed similar melting points as neat polymer at ~60 °C (Fig. 2b) during the first heating scan in DSC analysis, suggesting that PCL in the HME matrices remained crystalline, consistent with XRPD results. The enthalpy change was proportional to the polymer content in the matrices (Fig. 2b inset).

3.4. Meloxicam distribution in M/PCL HME matrices

Drug distribution in the M/PCL matrices was examined by SEM/EDX (Fig. 3). SEM showed that fresh M/PCL matrices were mostly solid with few pores (Fig. 3, supporting Fig. 9). Meloxicam, identified in the EDX

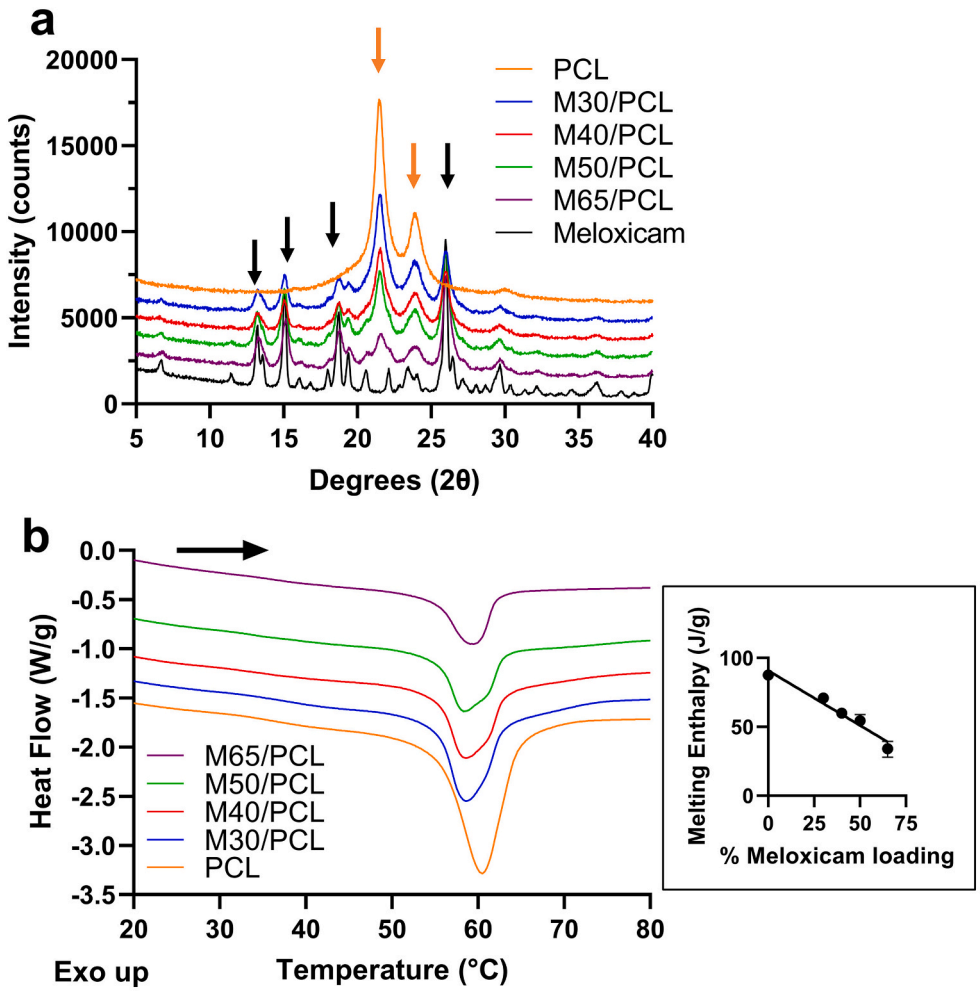

Fig. 2. (a) XPRD diffractograms (orange arrows: PCL peaks; black arrows: meloxicam peaks) and (b) DSC thermograms (primary heating scan) of meloxicam, PCL PC17, and HME PCL PC17 matrices with 30%, 40%, 50%, and 65% meloxicam loading. See Supporting Fig. 8 for cooling scan and second heating scan after cooling.

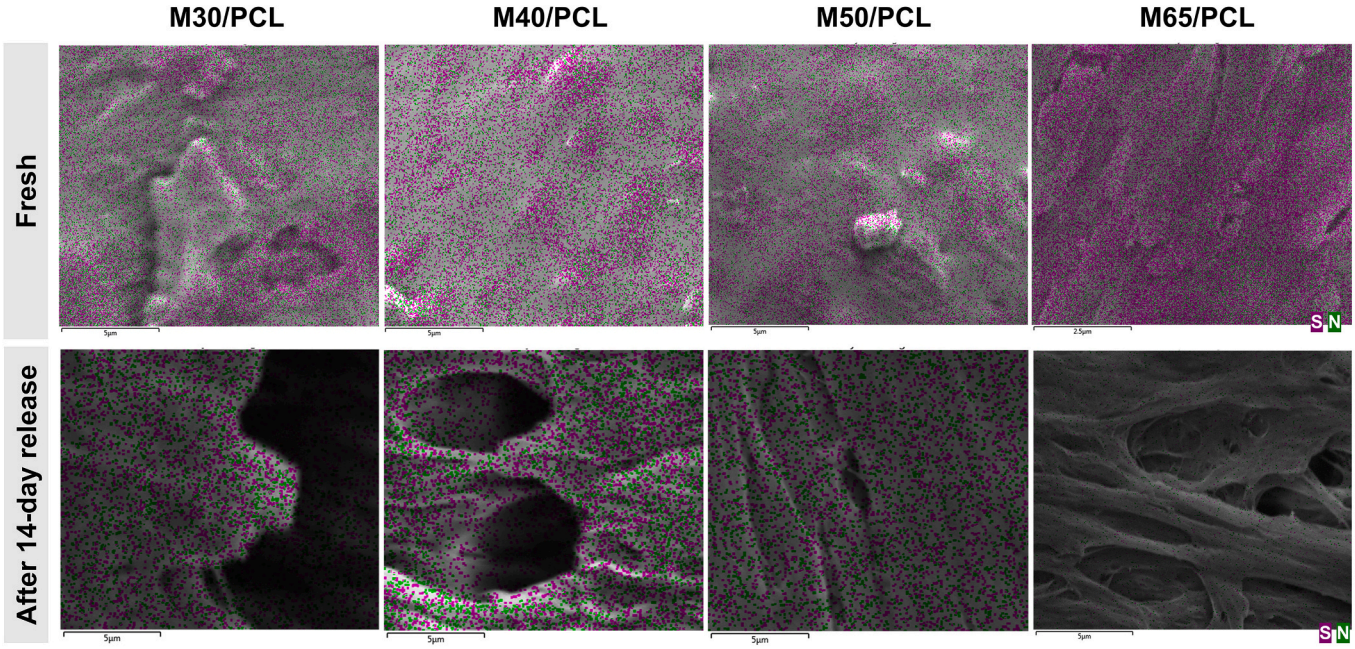

Fig. 3. SEM/EDX analysis of PCL PC17 matrices with 30, 40, 50 and 65 wt% meloxicam before and after *in vitro* drug release for 14 days (Sulfur: S, purple; nitrogen: N, blue). Scale bar = 5 μm. (For interpretation of the references to colour in this figure legend, the reader is referred to the web version of this article.)

mapping analysis (Fig. 3) by the presence of nitrogen (N) and sulfur (S), was found to be heterogeneously distributed in the matrices. The N and S signals increased with drug loading wt%. The ratio of S (meloxicam) to O (oxygen, contained in both meloxicam and polymer) in atomic frequency was proportional to the drug loading (wt%), but was 2–3 times higher than the theoretical ratio (based on 2S and 4O per meloxicam and 2O per PCL repeating unit) (Supporting Fig. 10); this may be attributable to the incomplete resolution of O from excess N, resulting in an underestimation of O. The heterogeneous drug distribution observed by EDX analysis (Fig. 3) and the crystallinity of HME matrices shown in XRPD (Fig. 2a, Supporting Fig. 7), taken together, suggest that meloxicam may be present as crystal clusters. MicroCT analysis was performed to complement the SEM/EDX analysis (Fig. 4). A cross-sectional grayscale image of fresh M65/PCL displayed porosity (black) and meloxicam clusters dispersed into PCL, where the grayscale corresponds to the density of each component, 1.19 g/cm^3 of PCL (dark-gray) and 1.69 g/cm^3 of meloxicam (bright-gray). These are classified as green and red labels, respectively, by AI segmentation (Fig. 4a, row 1). A visualized 3D reconstruction from the AI segmentation demonstrates that the meloxicam clusters were present throughout the matrix (Fig. 4b, left).

3.5. Meloxicam distribution in M/PCL HME matrices after drug release

M30/PCL, M40/PCL, M50 PCL, and M65/PCL were analyzed by SEM/EDX after the completion of 14-day drug release. EDX signals of S and N were barely seen in the matrices incubated for 14 days in PBST (Fig. 3, Supporting Fig. 10), resulting in negligible S/O ratio irrespective of drug loading. Given that the drug release from M30/PCL, M40/PCL, and M50/ PCL was incomplete by 14 days, the lack of meloxicam EDX signal in those matrices suggests preferential depletion of the drug in the surface layer. SEM detected pores generated in the matrix after the drug release (Fig. 3). Upon microCT scanning, M65/PCL after 14-day drug release showed no visible meloxicam clusters within the matrix but revealed large pores and an outer layer with low density, identified by red and yellow labels, respectively (Fig. 4a, row 2; Fig. 4b, right). The loose outer layer, likely swollen polymer, was estimated to be ~117 μm thick on average, according to the image analysis across the whole microCT scan (Supporting Fig. 11). BJH analysis was performed to quantify the porosity of the matrices after completing 14-day drug release. The porosity increased with the drug loading content (Fig. 5), suggesting that these pores were created following the dissolution and release of meloxicam crystal clusters.

3.6. Meloxicam pharmacokinetics from the subcutaneously implanted M/PCL HME matrices

To estimate the drug *in vivo* release rate, we first measured the plasma concentration profiles of meloxicam following the subcutaneous implantation of the M/PCL in rats (Fig. 6a). The subcutaneously implanted M/PCL matrices resulted in an average T_{max} between 24 h and 28.8 h (Fig. 6a), showing no statistically significant difference among the matrices. However, the extent of absorption and the overall bioavailability were different as indicated by the calculated dose-normalized C_{max} and AUC values, respectively (Table 2).

The *in vivo* meloxicam input profiles (Fig. 6b) were estimated by deconvoluting the subcutaneous plasma data (input-response function) based on the drug plasma concentration profile following an instantaneous absorption of a unit amount of drug (impulse-response function). IV bolus administration of meloxicam solution was used to calculate the UIR parameters according to the FDA guidance [44]. The IV plasma profiles were best fitted with a one-compartment PK model. Since the UIR is the response to one dose unit, for a one-compartment model, the inverse of the model parameter V was used for the UIR parameter A in Eq. 1. Therefore, A (1/V) was 1/0.057 (L^{-1}), and α (elimination rate constant) was 0.043 (h^{-1}). The deconvolution results calculate the input rate of the drug into the systemic circulation. Given the difference in the elimination phase between IV and subcutaneously administered drugs, we may not completely rule out the potential contribution of drug-tissue interaction to the input rate. However, meloxicam administered by a bolus subcutaneous injection quickly reached a drug plasma level comparable to IV administered drug (Fig. 6a), indicating that such an interaction would be minimal. Therefore, it is reasonable to consider that the input rate is largely dominated by the rate of drug release from the matrix and may be used to assess a correlation with *in vitro* drug release.

The deconvoluted *in vivo* input profiles of M/PCL HME matrices

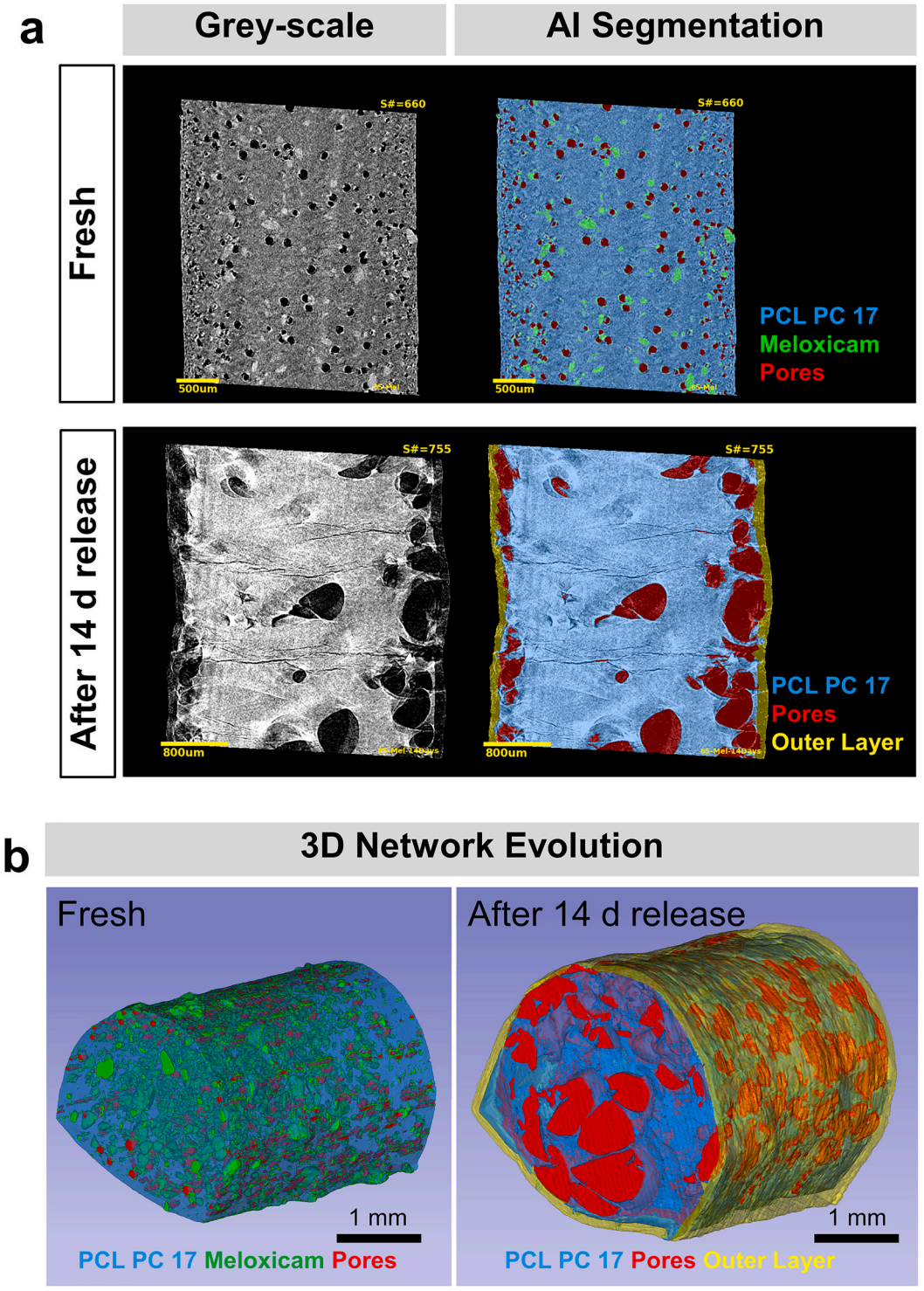

Fig. 4. (a) Grayscale longitudinal cross-sections and AI segmented cross-sections for M65/PCL matrices, fresh or incubated in PBST at 37 °C for 14 days for release study. Fresh cross-section image: black, porosity; dark-gray, PC17; bright-gray, meloxicam. After 14-day cross-section image: black, porosity; dark-gray, outer layer; gray, PC17. Scale bars: (row 1) 500 μm; (row 2) 800 μm. (b) 3D reconstructions of matrix networks using AI segmented microCT scans seen in a. 3D networks: blue, PC17; green, meloxicam; red, porosity; yellow, outer layer. Scale bars: 1 mm. (For interpretation of the references to colour in this figure legend, the reader is referred to the web version of this article.)

(Fig. 6b) followed the same rank order as their *in vitro* release profiles (Fig. 1b). Compared to the subcutaneous bolus dose arms, the M/PCL matrices clearly showed sustained meloxicam input. Of note, the percent *in vivo* input of meloxicam was lower than that of *in vitro*, where the estimated *in vivo* drug input was 30–50% of *in vitro* release (Supporting Fig. 12a). For all matrices, the estimated *in vivo* drug input and the unreleased drug (measured from the recovered matrices) added up to ~75% of the loaded drug (Supporting Fig. 12b).

3.7. IVIVC

IVIVC are predictive mathematical models that represent the

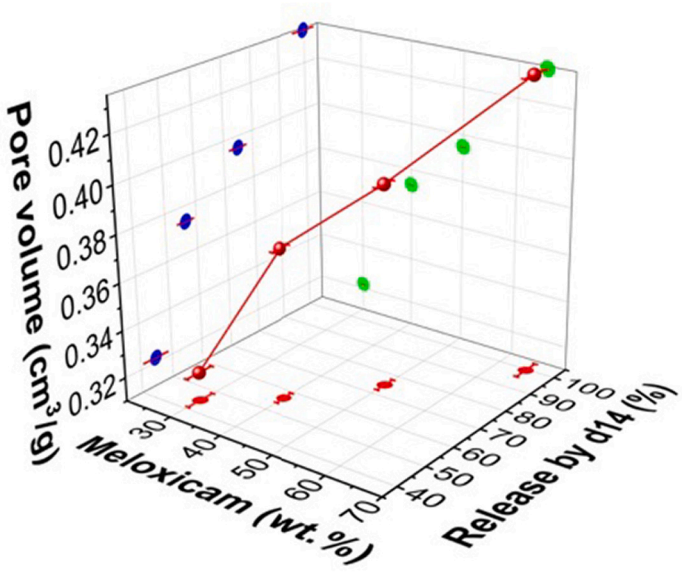

Fig. 5. Three-way relationship between meloxicam loading (wt%), cumulative meloxicam release by day 14, and pore volume (cm^3/g) measured in the M30/PCL, M40/PCL, M50/PCL and M65/PCL matrices after 14-day drug release.

relationship between an *in vitro* property such as dissolution and its *in vivo* performance such as plasma concentration. The deconvolution/convolution-based approach is commonly used to establish a level A IVIVC (a point-to-point relationship between the *in vitro* release and the *in vivo* input rate). The FDA guidance [44] recommends using a minimum of two, preferably three or more formulations with different release rates, to define an IVIVC of oral formulations. Applying this guidance to implantable systems, we used three formulations (M40/PCL, M50/PCL, and M65/PCL) to develop an IVIVC (see Supporting information for detailed analysis). M30/PCL was excluded because its drug release mechanism is suspected to be different than the others due to the relatively low drug content. We observed an affirmative Level A IVIVC between the fraction of drug released *in vitro* ($F_{rel,\ in\ vitro}$) and fraction of drug entering the system *in vivo* ($F_{input,\ in\ vivo}$) for the three matrices (Fig. 6c).

For the internal validation of the IVIVC, we compared the meloxicam plasma concentrations predicted from M40/PCL, M50/PCL, and M65/PCL with the observed plasma concentrations for each formulation (Supporting Fig. 13). The model predicted the plasma concentration profiles with the average absolute percent prediction error (%PE) for the internal validation of C_{max} and AUC of <20%.

3.8. Histological evaluation of implanted tissues

We examined the subcutaneous tissues implanted with M65/PCL to evaluate tissue responses to the implant comparing with normal tissues and those implanted with drug-free PCL matrices. Both implants showed mild to moderate infiltrate of mononuclear leukocytes, primarily composed of lymphocytes and plasma cells in deep dermis and subcutis near the implant sites (Supporting Fig. 14). Neither of them showed neutrophils or other signs of acute inflammation. There was no notable difference between the two implants.

4. Discussion

For prevention of inflammation and biofouling during post-surgical wound management, we designed a drug-eluting polymer matrix, consisting of a biocompatible polymer and meloxicam, a relatively selective COX-2 inhibitor. A primary design criterion was that the polymer matrix provides continuous meloxicam release for at least 14 days, a time frame critical to the prevention of inflammation and biofouling [45–49]. HME was used for combining the drug and polymer due to the capability of solvent-free processing and the adaptability to large scale production.

Three biocompatible polymers, PLGA, EVA, and PCL, were considered for controlling the release rate of meloxicam. *In vitro* drug release kinetics of HME matrices of meloxicam and polymer were first evaluated to determine the suitability of each polymer for the 14-day delivery of meloxicam (Fig. 1). PLGA and EVA were found to be unsuitable for controlled release of meloxicam, as neither of them released more than 11% or 36% of the total loaded drug in 14 days, with minimal effect of drug loading content on the total drug release (Supporting Fig. 3a). In both cases, there was no sign of drug degradation during the release kinetics study: the released and unreleased drugs from both PLGA and EVA matrices added up to ~100% of the loaded drug (Supporting Fig. 3b), and the HPLC peaks of meloxicam recovered from the matrices after release kinetics study were identical to fresh meloxicam (Supporting Fig. 3c). Therefore, the slow drug release from PLGA and EVA matrices may not be attributed to changes in drug stability. With M/EVA matrix, we speculate that the hydrophobicity of EVA may have interfered with the wetting of the matrix. Neat EVA matrix (without drug) showed a contact angle of 93.1°, and the addition of meloxicam did not lower the contact angle (101.9°). This observation suggests that the M/EVA matrix might have been initially resistant to wetting, although it showed a sign of slight wetting over time (Supporting Fig. 4), accounting for some drug release that was observed. In comparison, both PCL PC17 and PLGA RG502 showed a decrease in contact angle upon the addition of 30 wt% meloxicam (from 88.7° to 76° for PCL PC17; from 88.5° to 65.4° for PLGA RG502), and 7-day wetting in PBST further decreased the contact angle to 71.2° (M30/PCL PC17) and 58.2° (M30/PLGA RG502) (Supporting Fig. 2). Since PLGA matrix showed even better wetting than PCL matrix, we could not explain the limited meloxicam release from M/PLGA matrices as resulting from the hydrophobicity of the matrices. DSC thermograms showed no evidence of molecular interaction between meloxicam and PLGA RG502 indicative of drug affinity for the polymer (Supporting Fig. 1b). Instead, we suspect that the lack of drug release from the M/PLGA RG502 matrix may be at least partly explained by the decreased solubility of meloxicam due to the acidic microenvironment of the PLGA matrix. Meloxicam is an acidic drug (pKa = 1.1 and 4.6) with a relatively low solubility (< 3 μg/mL) at < pH 5 (Supporting Fig. 15a) [50]. Since the literature suggests the presence of residual monomers or oligomers in commercial PLGA [51], we recovered water-soluble impurities from the as-received PLGA

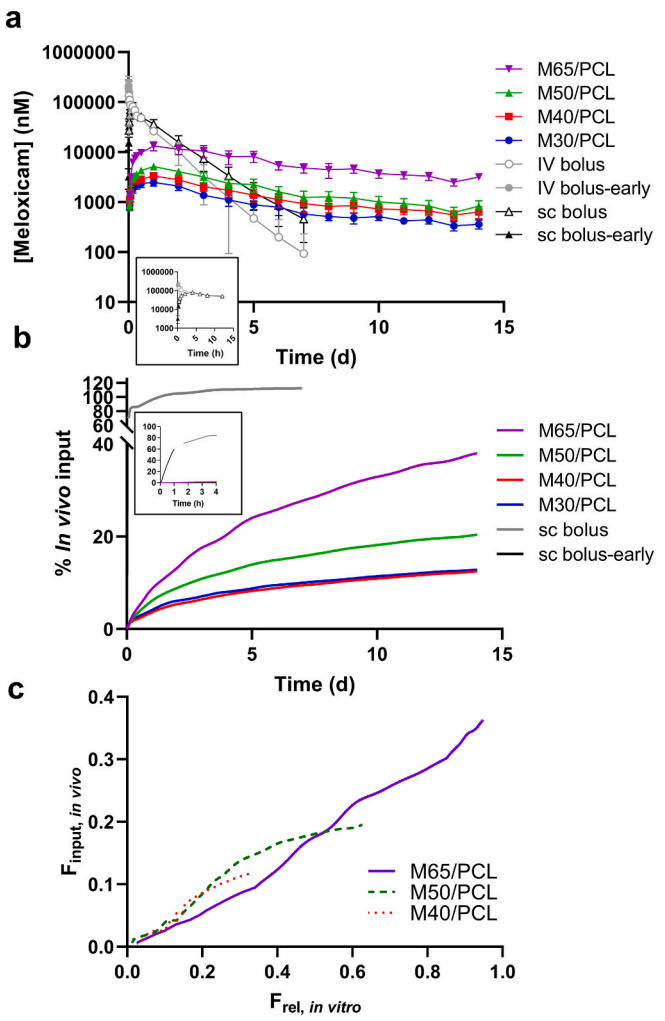

Fig. 6. (a) Mean plasma concentration-time profiles of meloxicam in rats following intravenous and subcutaneous administration of a meloxicam bolus solution and subcutaneous implantation of M/PCL matrices equivalent to 2.4–5.5 mg meloxicam. Mean ± SD, $n = 5$ independently and identically prepared batches. (b) % *in vivo* input of meloxicam post-subcutaneous administration of a single bolus solution and subcutaneous implantation of M/PCL matrices. (c) IVIVC developed with M40/PCL, M50/PCL, and M65/PCL matrices. $F_{input,\ in\ vivo}$: fraction of drug entering the system *in vivo*; $F_{rel,\ in\ vitro}$: fraction of drug released *in vitro*.

Table 2
Mean plasma PK parameters of meloxicam after subcutaneous implantation of M/PCL matrices in rats.

PK parameters	M30/PCL	M40/PCL	M50/PCL	M65/PCL
T_{max} (h) (CV%)	26	29 (37%)	24	29 (37%)
C_{max} (nM)/mg dose (CV%)	1054 (15%)	936 (11%)	1637 (8%)	2454 (20%)
AUC_{0-336} (nM*h)/mg dose (CV%)	130,982 (13%)	127,450 (20%)	208,585 (17%)	384,615 (20%)
Bioavailability (F, %)	13	13	21	39

RG502 polymer and M30/PLGA RG502 by liquid-liquid extraction and measured the pH. The water extract showed a pH less than 5 (Supporting Fig. 15b), suggesting that the water solubility of meloxicam entrapped in PLGA matrix would have been very low from the beginning due to the residual acidic impurities. The PLGA matrix would have become further acidified by hydrolysis during the incubation in PBST (Supporting Fig. 15c) and, thus, continued to prevent the dissolution of meloxicam.

In contrast, M/PCL matrices showed a continuous release of meloxicam over the course of 14 days. Compared to M/EVA, the facile meloxicam release from M/PCL matrices may be partly attributable to the wettability, which would have contributed to fluid infiltration and drug diffusion through the matrices. Unlike M/PLGA, M30/PCL did not generate an acidic microenvironment (Supporting Fig. 15c) in 14 days. PCL shows very slow degradation kinetics (total time of degradation: ~2 years for 112 kDa PCL PC17 [52]); therefore, polymer degradation is likely to be negligible over a 14-day time period. We exclude the difference in extrusion temperature (105–130 °C for PCL; 100–180 °C for PLGA; 150 °C for EVA) as a reason for the differential drug release, because drug release from the PLGA matrix was still limited after reducing the extrusion temperature to 100 °C or lower (data not shown). We also examined the internal structure of fresh M30/PCL and M30/PLGA by SEM to see if initial porosity (resulting from air pockets entrapped during the extrusion) may have affected the drug release rate. Prior to drug release studies, fresh M30/PLGA was more porous than M30/PCL (Supporting Fig. 16) but released meloxicam no more than 5% (Supporting Fig. 3), indicating that the initial porosity does not account for the relatively good drug release from M/PCL compared to M/PLGA.

The *in vitro* meloxicam release rate and % total drug release from M/PCL matrices increased with drug loading (Fig. 1b, c). Here, M/PCL matrices were loaded with meloxicam as solid crystalline particles that maintained their crystalline form throughout the extrusion process, as supported by XPRD, DSC, SEM/EDX and microCT. With a slow degradation rate, PCL matrix would have remained unchanged for 14 days; in the meantime, meloxicam crystals dissolved and diffused out of the matrix. The increased porosity after the 14-day drug release observed by SEM (Fig. 3) and microCT (Fig. 4) suggests that the dissolving crystals have generated fluid channels that facilitated additional drug dissolution and transport. The porosity of the M/PCL matrices after 14-day drug release increased in proportion to the drug loading content, further supporting the generation of drug-induced fluid channels (Fig. 5). High drug loading helped to increase the drug release rate because drug clusters may be interconnected better than those with lower drug loading as shown in image-based matrix analysis [53]. A similar trend was observed with an experimental HIV drug and a comparable set of polymers (PCL, PLA, and EVA), although the drug release rate was not affected by the polymer type in their study, likely due to the relatively high water solubility of the drug particles (1.35 mg/mL in PBS at 37 °C) [54]. The distribution of meloxicam clusters in M/PCL also played an important role in controlling drug release. M30/PCL prepared at a relatively high screw speed (200 rpm *vs.* standard 20 rpm), which helped to disperse the micronized meloxicam crystals in the matrix (Supporting Fig. 17a), showed a slower drug release than the typical M30/PCL matrix prepared with a screw speed of 20 rpm that had distinctive crystal clusters of meloxicam (Supporting Fig. 17b). This suggests that the improved dispersion of meloxicam crystals may have increased the chance to isolate the crystals and reduced the interconnectivity, especially for the matrices with relatively low drug loading.

The *in vivo* drug input rate estimated from PK profiles of subcutaneously implanted matrices showed a consistent trend with the *in vitro* release kinetics, with M65/PCL showing the largest fraction of drug release and *vice versa*. The extent of *in vivo* drug input was 30–50% of the *in vitro* drug release rate. A potential drug-tissue interaction may partly responsible for the difference, although the contribution is expected to be minimal given the fast subcutaneous drug absorption (Fig. 6a). This difference may also be explained by the artificial *in vitro* conditions for testing release kinetics. The drug release slowed down in a stagnant condition and accelerated in a release medium with a higher buffering capacity (hence better maintaining meloxicam solubility) (Supporting Fig. 18). This suggests that *in vivo* drug release is slower than the *in vitro* prediction due to the difference in the release medium and hydrodynamic conditions at the subcutaneous site. Therefore, in order to achieve 14-day release of meloxicam *in vivo*, the release rate needs to be increased beyond the current maximum with M65/PCL, which may be

achieved by additional meloxicam loading or the incorporation of porogens.

In summary, PCL HME matrices provide a platform for sustained delivery of meloxicam for 14 days. The drug embedded in the PCL matrix as crystalline clusters dissolves and diffuses out, leaving behind a porous network that generates fluid channels; thus, the release rate of meloxicam can be controlled by the drug to polymer weight ratio.

Acknowledgments

This study was supported by Eli Lilly and Company. The authors thank Prof. Jianguo Mei and Ms. Zhifan Ke at Purdue for the assistance with the contact angle measurement, Drs. Christopher L. Burcham, Paul A. Stroud, and Robert Behme at Lilly for the discussion of drug-polymer interactions, and John T. Catlow at Lilly for ADME support. The authors also appreciate the administrative support of Kaethe Beck, Drs. Thomas R. Verhoeven and James H. Parshall.

Appendix A. Supplementary data

Supplementary data to this article can be found online at https://doi.org/10.1016/j.jconrel.2021.12.038.

References

[1] E. Ricciotti, G.A. FitzGerald, Prostaglandins and inflammation, Arterioscler. Thromb. Vasc. Biol. 31 (2011) 986–1000.
[2] C. Hawkey, COX-1 and COX-2 inhibitors, best practice & research clinical, Gastroenterology 15 (2001) 801–820.
[3] W. Badri, K. Miladi, Q.A. Nazari, H. Greige-Gerges, H. Fessi, A. Elaissari, Encapsulation of NSAIDs for inflammation management: overview, progress, challenges and prospects, Int. J. Pharm. 515 (2016) 757–773.
[4] S. Wongrakpanich, A. Wongrakpanich, K. Melhado, J. Rangaswami, A comprehensive review of non-steroidal anti-inflammatory drug use in the elderly, Aging Dis. 9 (2018) 143.
[5] L. Baruch, O. Benny, A. Gilert, M. Ukobnik, O.B. Itzhak, M. Machluf, Alginate-PLL cell encapsulation system co-entrapping PLGA-microspheres for the continuous release of anti-inflammatory drugs, Biomed. Microdevices 11 (2009) 1103.
[6] S. Khanal, U. Adhikari, N.P. Rijal, S.R. Bhattarai, J. Sankar, N. Bhattarai, pH-responsive PLGA nanoparticle for controlled payload delivery of diclofenac sodium, Journal of functional biomaterials 7 (2016) 21.
[7] Y. Shi, Z. Liu, Y. Yang, X. Xu, Y. Li, T. Li, Design of poly (mPEGMA-co-MAA) hydrogel-based mPEG-b-PCL nanoparticles for oral meloxicam delivery, Mater. Sci. Eng. C 76 (2017) 975–984.
[8] H. Paukkonen, M. Kunnari, P. Laurén, T. Hakkarainen, V.-V. Auvinen, T. Oksanen, R. Koivuniemi, M. Yliperttula, T. Laaksonen, Nanofibrillar cellulose hydrogels and reconstructed hydrogels as matrices for controlled drug release, Int. J. Pharm. 532 (2017) 269–280.
[9] M.F. Canbolat, A. Celebioglu, T. Uyar, Drug delivery system based on cyclodextrin-naproxen inclusion complex incorporated in electrospun polycaprolactone nanofibers, Colloids Surf. B: Biointerfaces 115 (2014) 15–21.
[10] J. Pang, Y. Luan, F. Li, X. Cai, J. Du, Z. Li, Ibuprofen-loaded poly (lactic-co-glycolic acid) films for controlled drug release, Int. J. Nanomedicine 6 (2011) 659.
[11] R. Fleischmann, I. Iqbal, P. Nandeshwar, A. Quiceno, Safety and efficacy of disease-modifying anti-rheumatic agents, Drug Saf. 25 (2002) 173–197.
[12] J.V. Roughan, H.G. Bertrand, H.M. Isles, Meloxicam prevents COX-2-mediated post-surgical inflammation but not pain following laparotomy in mice, Eur. J. Pain 20 (2016) 231–240.
[13] G. Engelhardt, Pharmacology of meloxicam, a new non-steroidal anti-inflammatory drug with an improved safety profile through preferential inhibition of COX-2, Rheumatology 35 (1996) 4–12.
[14] D.E. Furst, Meloxicam: selective COX-2 inhibition in clinical practice, in: Seminars in Arthritis and Rheumatism, Elsevier, 1997, pp. 21–27.
[15] B. Xin, Y. Yokoyama, T. Shigeto, H. Mizunuma, Anti-tumor effect of non-steroidal anti-inflammatory drugs on human ovarian cancers, Pathology & Oncology Research 13 (2007) 365–369.
[16] T. Li, J. Zhong, X. Dong, P. Xiu, F. Wang, H. Wei, X. Wang, Z. Xu, F. Liu, X. Sun, Meloxicam suppresses hepatocellular carcinoma cell proliferation and migration by targeting COX-2/PGE2-regulated activation of the β-catenin signaling pathway, Oncol. Rep. 35 (2016) 3614–3622.
[17] P. She, Y. Wang, Z. Luo, L. Chen, R. Tan, Y. Wang, Y. Wu, Meloxicam inhibits biofilm formation and enhances antimicrobial agents efficacy by Pseudomonas aeruginosa, MicrobiologyOpen 7 (2018), e00545.
[18] N. PHARMA, ANDA211398 MELOXICA, CAPSULE;ORAL, in: U.S.F.a.D. Administration, 2018.
[19] T.T. LLC, NDA211210 QMIIZ ODT (MELOXICAM), TABLET, ORALLY DISINTEGRATING;ORAL, in: U.S.F.a.D. Administration (Ed.), 2018.
[20] ZYLA, NDA207233 VIVLODEX (MELOXICAM), CAPSULE;ORAL, 2015.
[21] L. LTD, ANDA209487 MELOXICAM, CAPSULE;ORAL, in: U.S.F.a.D. Administration (Ed.), 2020.
[22] B.B. Inc, ANJESO (Meloxicam), SOLUTION;INTRAVENOUS, in: U.S.F.a.D. Administration (Ed.), 2020.
[23] B.T. Hospital, NCT04322175 pharmacokinetic and tolerance study of meloxicam eye drops in healthy volunteers, in: U.S.N.L.o. Medicine, 2020.
[24] L.A. S.A, NCT02255045 Assessment of a Vaginal Ring With Meloxicam in the Treatment of Dysmenorrhea, in: U.S.N.L.o. Medicine, 2014, p. 2018.
[25] A.U. Ahmed Mohamed Abbas, NCT03146000 Lidocaine-prilocaine Cream Versus Rectal Meloxicam on Relief of Post-episiotomy Pain, in: U.S.N.L.o. Medicine, 2017.
[26] A.A. Kassem, F.A. Ismail, V.F. Naggar, E. Aboulmagd, Comparative study to investigate the effect of meloxicam or minocycline HCl in situ gel system on local treatment of periodontal pockets, AAPS PharmSciTech 15 (2014) 1021–1028.
[27] H.P. Sandoval, L.E.F. de Castro, D.T. Vroman, K.D. Solomon, A review of the use of ketorolac tromethamine 0.4% in the treatment of post-surgical inflammation following cataract and refractive surgery, Clinical Ophthalmology (Auckland, NZ) 1 (2007) 367.
[28] N. Fernández, E.E. Díaz, R. Amils, J.L. Sanz, Analysis of microbial community during biofilm development in an anaerobic wastewater treatment reactor, Microb. Ecol. 56 (2008) 121–132.
[29] S. Zhang, A.P. Byrnes, J. Jankovic, J. Neilly, Management, analysis, and simulation of micrographs with cloud computing, Microscopy Today 27 (2019) 26–33.
[30] H. Xi, A. Zhu, G.R. Klinzing, L. Zhou, S. Zhang, A.J. Gmitter, K. Ploeger, P. Sundararajan, M. Mahjour, W. Xu, Characterization of spray dried particles through microstructural imaging, J. Pharm. Sci. 109 (2020) 3404–3412.
[31] A. Fedorov, R. Beichel, J. Kalpathy-Cramer, J. Finet, J.-C. Fillion-Robin, S. Pujol, C. Bauer, D. Jennings, F. Fennessy, M. Sonka, 3D slicer as an image computing platform for the quantitative imaging network, Magn. Reson. Imaging 30 (2012) 1323–1341.
[32] D.J. Phillips, S.R. Pygall, V.B. Cooper, J.C. Mann, Overcoming sink limitations in dissolution testing: a review of traditional methods and the potential utility of biphasic systems, J. Pharm. Pharmacol. 64 (2012) 1549–1559.
[33] B. Vaghela, R. Kayastha, N. Bhatt, N. Pathak, D. Rathod, Development and validation of dissolution procedures, Journal of applied pharmaceutical science 1 (2011) 50–56.
[34] U. Pharmacopeia, USP-NF<1092> THE DISSOLUTION PROCEDURE: DEVELOPMENT AND VALIDATION, USP 32-NF27, 2009.
[35] U. Pharmacopeia, USP-NF< 1225> Validation of Compendial Methods, USP 32-NF27, 2009.
[36] E.P. Barrett, L.G. Joyner, P.P. Halenda, The determination of pore volume and area distributions in porous substances. I. Computations from nitrogen isotherms, J. Am. Chem. Soc. 73 (1951) 373–380.
[37] N. Genina, J. Holländer, H. Jukarainen, E. Mäkilä, J. Salonen, N. Sandler, Ethylene vinyl acetate (EVA) as a new drug carrier for 3D printed medical drug delivery devices, Eur. J. Pharm. Sci. 90 (2016) 53–63.
[38] C. Schneider, R. Langer, D. Loveday, D. Hair, Applications of ethylene vinyl acetate copolymers (EVA) in drug delivery systems, J. Control. Release 262 (2017) 284–295.
[39] E. Malikmammadov, T.E. Tanir, A. Kiziltay, V. Hasirci, N. Hasirci, PCL and PCL-based materials in biomedical applications, J. Biomater. Sci. Polym. Ed. 29 (2018) 863–893.
[40] P. Blasi, Poly (lactic acid)/poly (lactic-co-glycolic acid)-based microparticles: an overview, Journal of Pharmaceutical Investigation (2019) 1–10.
[41] K. Park, S. Skidmore, J. Hadar, J. Garner, H. Park, A. Otte, B.K. Soh, G. Yoon, D. Yu, Y. Yun, Injectable, long-acting PLGA formulations: analyzing PLGA and understanding microparticle formation, J. Control. Release 304 (2019) 125–134.
[42] J.R. Hughey, J.M. Keen, C. Brough, S. Saeger, J.W. McGinity, Thermal processing of a poorly water-soluble drug substance exhibiting a high melting point: the utility of KinetiSol(R) dispersing, Int. J. Pharm. 419 (2011) 222–230.
[43] P.J. Marsac, T. Li, L.S. Taylor, Estimation of drug–polymer miscibility and solubility in amorphous solid dispersions using experimentally determined interaction parameters, Pharm. Res. 26 (2009) 139–151.
[44] FDA, Guidance for Industry: Extended Release Oral Dosage Forms: Development, Evaluation, and Application of In Vitro/In Vivo Correlations, FDA, 1997.
[45] P. Gupta, S. Sarkar, B. Das, S. Bhattacharjee, P. Tribedi, Biofilm, pathogenesis and prevention—a journey to break the wall: a review, Arch. Microbiol. 198 (2016) 1–15.
[46] N. Wisniewski, M. Reichert, Methods for reducing biosensor membrane biofouling, Colloids Surf. B: Biointerfaces 18 (2000) 197–219.
[47] W. Zimmerli, P. Sendi, Orthopaedic biofilm infections, Apmis 125 (2017) 353–364.
[48] R.R. Doshi, J.F. Arevalo, H.W. Flynn Jr., E.T. Cunningham Jr., Evaluating exaggerated, prolonged, or delayed postoperative intraocular inflammation, Am J. Ophthalmol. 150 (2010) (295-304. e291).
[49] M. Sedlář, J. Kvasnička, Z. Krška, T. Tománková, A. Linhart, Early and subacute inflammatory response and long-term survival after hip trauma and surgery, Arch. Gerontol. Geriatr. 60 (2015) 431–436.
[50] P. Sieger, Y. Cui, S. Scheuerer, pH-dependent solubility and permeability profiles: a useful tool for prediction of oral bioavailability, Eur. J. Pharm. Sci. 105 (2017) 82–90.
[51] M. Kohno, J.V. Andhariya, B. Wan, Q. Bao, S. Rothstein, M. Hezel, Y. Wang, D. J. Burgess, The effect of PLGA molecular weight differences on risperidone release from microspheres, Int. J. Pharm. 582 (2020), 119339.

[52] M. Bartnikowski, T.R. Dargaville, S. Ivanovski, D.W. Hutmacher, Degradation mechanisms of polycaprolactone in the context of chemistry, geometry and environment, Prog. Polym. Sci. 96 (2019) 1–20.
[53] D. Skomski, Z. Liu, Y. Su, C.T. John, A. Doty, S.P. Forster, R. Teller, S.E. Barrett, W. Xu, An imaging toolkit for physical characterization of long-acting pharmaceutical implants, J. Pharm. Sci. 109 (2020) 2798–2811.
[54] S.E. Barrett, R.S. Teller, S.P. Forster, L. Li, M.A. Mackey, D. Skomski, Z. Yang, K. L. Fillgrove, G.J. Doto, S.L. Wood, Extended-duration MK-8591-eluting implant as a candidate for HIV treatment and prevention, Antimicrob. Agents Chemother. 62 (2018) (e01058-01018).